Peer-reviewed version available at Mar. Drugs 2019, 17, 624; doi:10.3390/md17110624

Article

Computational Tools in the Discovery of FABP4 Ligands: A Statistical and Molecular Modeling Approach

Giuseppe Floresta [1,*], Davide Gentile [1], Giancarlo Perrini [2], Vincenzo Patamia [1] and Antonio Rescifina [1,3,*]

[1] Department of Drug Sciences, University of Catania, V.le A. Doria, 95125 Catania, Italy; giuseppe.floresta@unict.it (G.F.), davide.gentile@unict.it (D.G.), vincenzo.patamia@unict.it (V.P.) and arescifina@unict.it (A.R.)
[2] Department of Chemical Sciences, University of Catania, V.le A. Doria, 95125 Catania, Italy; gperrini@unict.it (G.P.),
[3] Consorzio Interuniversitario Nazionale di ricerca in Metodologie e Processi Innovativi di Sintesi (C.I.N.M.P.S.), Via E. Orabona, 4, 70125 Bari, Italy; arescifina@unict.it (A.R.)
* Correspondence: giuseppe.floresta@unict.it (G.F.) and arescifina@unict.it (A.R.)

Abstract: Small molecule inhibitors of adipocyte fatty-acid binding protein 4 (FABP4) have got interest following the recent publication of their pharmacologically beneficial effects. Recently it comes out that FABP4 is an attractive molecular target for the treatment of type 2 diabetes, other metabolic diseases, and some type of cancers. In the past years, hundreds of effective FABP4 inhibitors have been synthesized and discovered but, unfortunately, none of them is in the clinical research phase. The field of computer-aided drug design seems to be promising and useful for the identification of FABP4 inhibitors; hence, different structure- and ligand-based computational approaches were already performed for their identification. In this paper, we searched for new potentially active FABP4 ligands in the Marine Natural Products (MNP) database. 14,492 compounds were retrieved from this database and filtered through a statistical and computational filter. Seven compounds were suggested by our methodology to possess a potential inhibitory activity upon FABP4 in the range of 79–245 nM. ADMET properties prediction were performed to validate the hypothesis of the interaction with the intended target and to assess the drug-likeness of these derivatives; from these analyses, three molecules resulted as excellent candidates for becoming new drugs.

Keywords: FABP4, A-FABP, aP2, antidiabetes, antiobesity, antiatherosclerosis, anticancer, computational tools, computer-aided drug discovery.

1. Introduction

Fatty acids (FAs) are a class of carboxylic acids that have many functions of vital importance in humans [1]. It was recently reported that elevated levels of FAs in plasma lead to specific physiological disorders [2], among these is worth remember type 2 diabetes [3], obesity [4] and atherosclerosis [5]. FAs have poor solubility in water, to overcome the problem they are always associated with carrier proteins to facilitate the trafficking in aqueous environments. Some examples of these carrier proteins are albumin, lipocalins, and fatty acid-binding proteins (FABPs) [6].

The adipocyte FABP (also called A-FABP, aP2, or FABP4) is the highly expressed FABPs in adipocytes; its levels are regulated by the peroxisome-proliferator-activated receptor-c agonists, as well as by the levels of insulin and by the level of free FAs [7]. Studies conducted in FABP4 knockout mice have shown that this carrier protein has a crucial role in many aspects of the metabolic syndrome

Peer-reviewed version available at Mar. Drugs 2019, 17, 624; doi:10.3390/md17110624

[8, 9], with a potential impact for the future clinical treatments of this disorder. Indeed, the lack of the gene that codifies for FABP4 partially prevents the advancement of insulin resistance and obesity in mice. Thus, small-molecules that inhibit the physiological function of FABP4 can mimic the phenotype of FABP4-deficient mice and might be useful candidates for the treatment of metabolic syndromes. It was also reported that FABP4 is highly expressed in macrophages [10]. Macrophages are an essential site of FABPs action, and total or macrophage-specific FABP4-deficiency leads to a marked defense against early and advanced atherosclerosis [11].

The family of FABPs proteins has also a significant role in the cancer cell and cancer progression [12]. Up to now, modified FABPs expressions were described for different types of cancers like prostate, bladder, renal cell carcinoma, and other types of cancer cells [13-15]. Despite this, FABPs biological functions in cancer remain mostly unclear [16].

Recently, a variety of effective FABP4 inhibitors have been developed [17] but, unfortunately, none of them is currently in the clinical research phases (Figure 1).

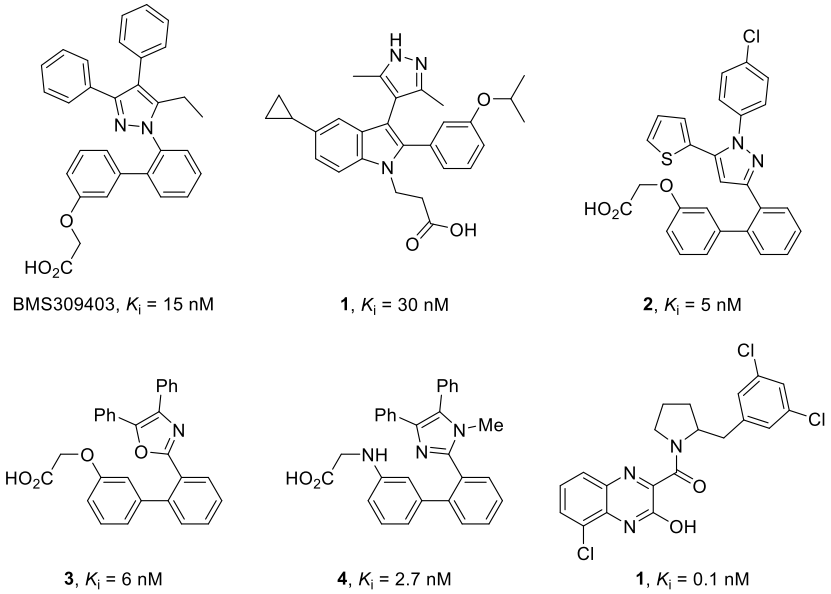

Figure 1. Structures of selected potent FABP4 inhibitors belonging to various chemical classes.

Computer-aided drug design shows a promising and useful tool for the identification of novel molecules able to bind FAPB4. Notably, different structure-based computational approaches (docking based virtual screening studies) have been already performed in this context with different libraries of compounds, leading to important results [18, 19].

In line with our recent interest in the development of QSAR models and related applications [20-27], we recently produced the first 3D-QSAR model for the description of a dataset of selective and potent FABP4 inhibitors [28, 29]. The 3D-QSAR model was then combined with a scaffold-hopping analysis, allowing the design of new potent molecules able to interact with the binding site and inhibit the FABP4; finally, three of the ligands suggested by the scaffold-hopping analysis were synthesized and tested *in vitro* yielding IC_{50} values between 3.70 and 5.59 μM.

Given the excellent result in identifying novel structures and in assisting in the design of novel FABP4 binder of this 3D-QSAR model, in this work, we decided to combine the ligand-based approach with a structure-based one (docking) to screen a large dataset of marine product for the identification of novel hit-compounds among the marine word. This purpose has been pursued employing a statistical and computational approach as already successfully reported for the identification of sigma-2 receptor ligands [30] and heme oxygenase 1 inhibitors [31].

2. Results

2.1. Design and application of the three filters used for the MNP database screening

The first filter used for the identification of FABP4 ligands was a statistical (based on 2D and 3D descriptors) one, as already used successfully by us [31]. 2,922 molecules were selected among the MNP database by a statistical/2D descriptors filter using DataWarrior software [32]. The appropriate range of values to be considered for each chosen descriptor was obtained analyzing the most potent and selective compounds present in a recently published dataset of FABP4 ligands for a total of 120 entities [28, 29]. So, the ranges for molecular weight (MW, 224/501), cLogP (−0.84/6.1.), cLogS (−8.77/−2.33), H-bond-acceptors (HBA, 2/7), H-bond-donors (HBD,0/2), total surface area (TSA, 170/400), polar surface area (PSA, 40/125), and relative polar surface area (RPSA, 0.07/0.4) (Figure 2), belonging to the 120 potent and selective FABP4 inhibitors, were associated to each descriptor and applied to the dataset of 14,492 MNP molecules to give 2,922 marine filtered compounds.

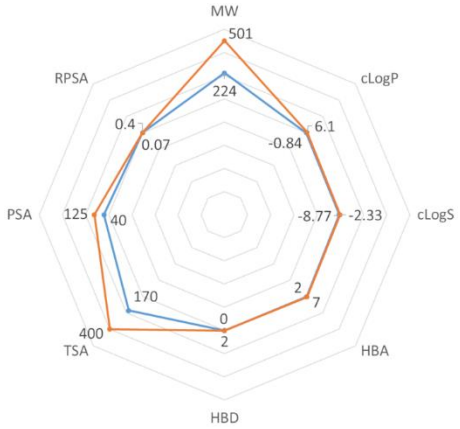

Figure 2. Radar plot representation of the ranges values (minimum in blue and maximum in orange) of the eight selected descriptors associated with the 120 FABP4 inhibitors.

These skimmed molecules were then subjected to a second filtration using a mixed ligand- and structure-based approach. Firstly, the 3D molecular structures of the 2,922 marine compounds were aligned to our previous published 3D-QSAR model for the FABP4 protein, and the compounds were then evaluated, as previously reported, employing Forge software (v10.4.2, Cresset, New Cambridge House, United Kingdom) [33]. Over the whole dataset of the first filtered marine natural products, 1854 molecules resulted in an excellent or good description by the model. This means that most of the features in the evaluated molecules were well described by the training set of the 3D-QSAR model, and the predicted activity can be considered reliable. Among these compounds, 198 molecules resulted in a predicted pIC_{50} activity between 6.0 and 7.6. The 3D molecular structures of the 2,922 marine compounds were then passed to the structure-based approach adapting the docking procedure already reported for the identification of FABP4 inhibitors [34, 35]. The AutoDock Vina software (v. 1.1.2, Molecular Graphics Lab at The Scripps Research Institute, La Jolla, California) [36] was used for all docking studies. The validation of the adopted docking procedure was assessed employing the Pearson's correlation coefficient method upon a benchmark data set of 34 known FABP4 inhibitors (Table S1, Figure S1).

After the calculations with AutoDock Vina, all the generated structures were manually inspected, in order to ensure a correct positioning within the binding pocket. The 3D-QSAR and docking evaluation results are reported in Table S2.

2.2. Merged ligand- and structure-based filters

The results derived from the ligand-based calculation (*i.e.*, 3D-QSAR evaluation) and the structure-based calculation (*i.e.*, docking calculations) were then merged with the aim to create a final filter. For this purpose, the best (lowest calculated IC_{50} or K_i) 2% and 5% of the molecules obtained from each of the two approaches were retrieved, and those simultaneously present in both filters have been selected (Table 1). The 2% filter resulted in only one molecule (5339) whereas the 5% one returned other six molecules (14123, 13575, 7846, 3164, 2076 and 1534).

Peer-reviewed version available at Mar. Drugs 2019, 17, 624; doi:10.3390/md17110624

Table 1. Structure, calculated pIC_{50} and pK_i, and their mean, of the selected marine products.

MNP ID	Structure	pIC_{50} (QSAR)	pK_i (Docking)	Mean
5339[a]	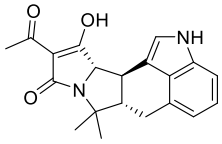	6.40	7.79	7.10
14123[b]	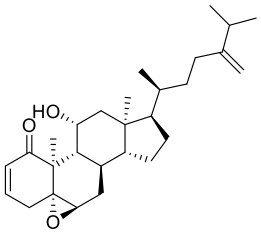	6.30	7.39	6.85
13575[b]	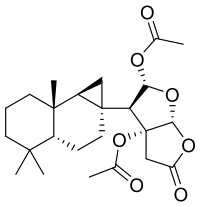	6.10	7.92	7.01
7846[b]	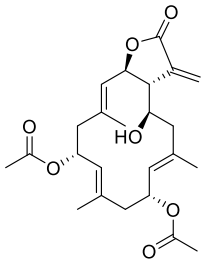	6.40	7.30	6.85
3164[b]	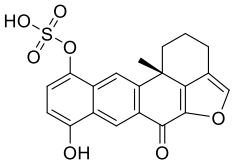	6.30	7.25	6.78
2076[b]	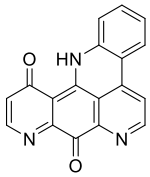	6.10	7.42	6.76
1534[b]	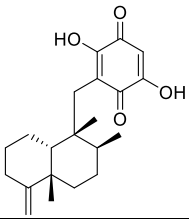	6.10	7.11	6.61

[a] Present in the first 2% of both ligand- and structure-based filters. [b] Present in the first 5% of both ligand- and structure-based filters.

All the binding poses retrieved from the molecular docking calculations of the seven compounds reported in Table 1, that showed the classical interactions of the most common FABP4 ligands, are reported in the supplementary material (Figures S2–S8). In particular, the best-docked pose of compound 5339, chosen as representative, superposed with the co-crystallized structure of the BMS309403 FABP4 inhibitor in the binding pocket the protein shows that the two compounds are partially overlapped and occupy almost the totality of the orthosteric site (Figure 3).

Peer-reviewed version available at Mar. Drugs 2019, 17, 624; doi:10.3390/md17110624

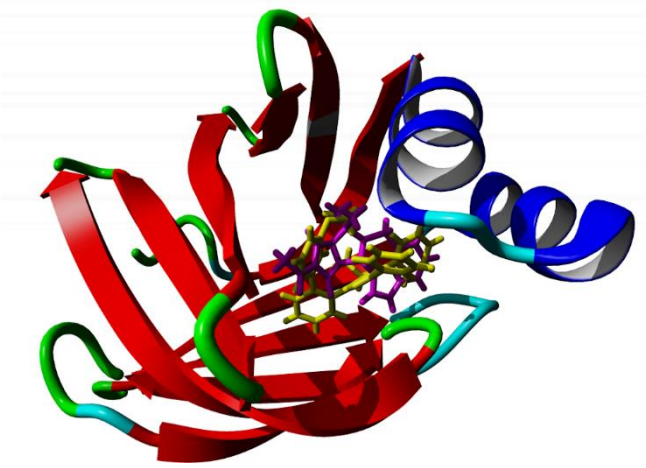

Figure 3. Best-docked pose of compounds 5339 (magenta) superposed with the co-crystallized structure of the BMS309403 (yellow) FABP4 inhibitor in the binding pocket of the protein (PDB ID: 2NNQ).

Among the seven filtered best potential inhibitors, molecule 5339 (indole alkaloid) has been reported as an inhibitor of Ca^{2+}-ATPase of the sarcoendoplasmic reticulum (SERCA) [37]. Compound 14123 (steroid) was identified as cytotoxic and anti-tumor [38]. Compound 13575 (diterpene) was tested for its cytotoxicity against several tumor cells, but it lacked any activity [39]. 7846 is a cembrane diterpenoid; similar compounds were reported to exert growth-inhibition effects toward tumor cells [40]. 3164 (pentacyclic hydroquinone) was reported as cytotoxic by acting in the DNA topoisomerase I [41]. Compound 2076 (alkaloid) was reported as cytotoxic against several tumor cell lines [42]. Compound 1534 (sesquiterpene) has anti-inflammatory activity by acting as Phospholipase A2 (PLA2) inhibitor [43]. Interestingly, PLA2 catalyzes the hydrolysis of phospholipids to produce free fatty acids. The fatty acid is the substrate for the biosynthesis of eicosanoids that are known to mediate inflammation. Based on this mode of action, compounds that inhibit PLA2 activity have been targeted as potential therapeutic agents in the treatment of inflammation. It was already proved the association between PLA2 and FABP4 in the regulation of inflammatory responses [44], and dual inhibition of such proteins would be advantageous in inflammation treatment. Moreover, compound 1534 is a sesquiterpene, and this class of natural products together with steroids, diterpenes, diterpenoids, quinones, and alkaloids was already identified as candidates for the inhibition of FABP4 [45].

2.3. ADMET properties

Since the interaction of an inhibitor with an enzyme/protein cannot guarantee its suitability as a drug, to further strengthen the results of 3D-QSAR and docking studies, we also performed *in silico* ADMET studies on the seven molecules reported in Table 1. The ability to reach targets in bioactive form was assessed using the SwissADME (http://swissadme.ch) and pkCSM (http://biosig.unimelb.edu.au/pkcsm/) web platforms. Importantly, the technologies implemented in these platforms are able to predict, with a fair degree of certainty, the false-positive results commonly observed in biochemical assays of small molecules [46].

The oral availability of our proposed bioactive compounds is shown in the bioavailability radar plots (Figure 4), which provide a graphical snapshot of the drug-likeness parameters of the investigated molecule. Notably, five compounds (5339, 13575, 7846, 3164, and 1534) have been predicted as orally bioavailable whereas compounds 14123 and 2076 presents only one off-shoot relative to the lipophilicity (LIPO) and unsaturation (INSATU) vertexes, respectively, leading to suboptimal physicochemical properties for their oral bioavailability.

Preprints (www.preprints.org) | NOT PEER-REVIEWED | Posted: 5 September 2019 doi:10.20944/preprints201909.0063.v1

Peer-reviewed version available at Mar. Drugs 2019, 17, 624; doi:10.3390/md17110624

Figure 4. Radar plots of the six drug-likeness parameters used to predict the oral bioavailability of the seven investigated compounds. The colored zone is a suitable physicochemical space for oral bioavailability. LIPO (Lipophility): −0.7 < XLOGP3 < 5.0; SIZE: 150g/mol < MW < 500g/mol; POLAR (Polarity): 20 Å^2 < TPSA < 130 Å^2; INSOLU (Insolubility): 0 < Log *S* (ESOL) < 6; INSATU (Insaturation): 0.25 < Fraction Csp^3 < 1; FLEX (Flexibility): 0 < Num. rotatable bonds < 9. All results have been obtained from the SwissADMET web server [47].

In addition to the Lipinski rule of five [48], other four drug-likeness rules named Ghose [49], Egan [50], Veber [51], and Muegee [52], have been contemporarily satisfied by six compounds with the exception of molecule 14123 (Table 2). Instead, the stringent lead-like criteria of Teague [53] have been passed by compounds 5339 and 2076. Since lead-likeness tests are intended to provide leads with high affinity in high-throughput screens that allow for the discovery and exploitation of additional interactions in the lead-optimization phase, molecules 5339 and 2076 are excellent candidates to be investigated based on scaffold hopping approach.

Finally, the outcome of the pan assay interference structures (PAINS) model [54], conceived to exclude small molecules that are likely to show false positives in biological assays, post only one alert for compound 1534, concerning the presence of a quinone moiety.

Table 2. Drug-likeness, lead-likeness, and PAINS parameters of compounds reported in Table 1[a].

MNP ID		5339	14123	13575	7846	3164	2076	1534
Drug-likeness	Lipinski violations	0	1	0	0	0	0	0
	Ghose violations	0	2	0	0	0	0	0
	Veber violations	0	0	0	0	0	0	0
	Egan violations	0	0	0	0	0	0	0
	Muegge violations	0	1	0	0	0	0	0
Lead-likeness violations		0	2	2	1	2	0	1
PAINS alerts		0	0	0	0	0	0	1

[a] All results have been obtained from the SwissADMET web server [47].

Human gastrointestinal absorption (HIA) and blood-brain barrier penetration (BBB), relative to the absorption and distribution parameters, respectively, have been graphically represented by the extended and renewed version of the Edan-Egg model named Brain Or IntestinaL EstimateD (BOILED) permeation predictive model (BOILED-Egg). The visual analysis of Figure 5 highlights that all investigated molecules, with the exception of 3164, have been predicted to be passively absorbed by the gastrointestinal tract, and three of them, 5339, 14123, and 2076, passively permeate through

Preprints (www.preprints.org) | NOT PEER-REVIEWED | Posted: 5 September 2019 doi:10.20944/preprints201909.0063.v1

Peer-reviewed version available at Mar. Drugs 2019, 17, 624; doi:10.3390/md17110624

the BBB, the first with the aid of the P-glycoprotein and the other two without it. These data are reflected in the values shown in Table 3.

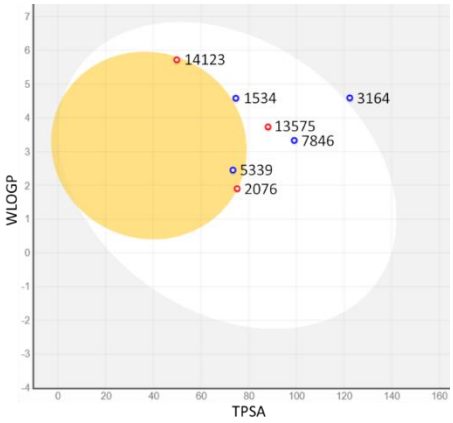

Figure 5. BOILED-Egg plot. Points located in the BOILED-Egg's yolk (yellow) represent the molecules predicted to passively permeate through the blood-brain barrier (BBB), whereas the ones in the egg white are relative to the molecules predicted to be passively absorbed by the gastrointestinal tract; the blue dots indicate the molecules for which it was expected to be effluated from the central nervous system (CNS) by the P-glycoprotein, whereas the red ones point-out to the molecules predicted not to be effluated from the CNS by the P-glycoprotein.

Regarding the absorption parameters. compounds 5339, 14123, 13575, and 2076 present a promising oral availability, due to the optimal Caco-2 cell permeability and HIA (> 0.9 and > 90%, respectively, Table 3), and skin permeability (logK_p < −2.5, Table 3).

Table 3. Pharmacokinetic and toxicity evaluated parameters of compounds reported in Table 1[a,b].

	MNP ID	5339	14123	13575	7846	3164	2076	1534
Absorption	Caco-2 permeability	0.967	1.318	1.700	0.916	−0.363	1.236	0.596
	Human intestinal absorption	92.279	95.061	97.33	88.869	68.223	98.368	91.388
	Skin permeability	−3.198	−2.864	−2.829	−3.486	−2.735	−2.895	−3.482
Distribution	VD_{ss} (human)	0.458	−0.177	0.031	−0.276	−1.88	0.145	−0.014
	Fraction unbound (human)	0.157	0.000	0.055	0.338	0.021	0.029	0.067
	BBB permeability	0.536	0.016	−0.707	−0.616	−0.802	0.021	−0.053
	CNS permeability	−2.124	−1.628	−2.183	−2.859	−3.041	−2.176	−1.869
Excretion	Total clearance	0.553	0.501	0.228	1.374	0.181	0.444	0.925
	Renal OCT2 substrate[b]	No	No	Yes	No	No	No	No
Toxicity	AMES toxicity	No	No	No	No	No	Yes	No
	Oral rat acute toxicity (LD_{50})	2.564	2.175	2.119	2.823	2.664	2.305	2.341
	Minnow toxicity	−0.338	−0.467	0.169	2.126	−0.189	0.260	0.038

[a] All results have been obtained from the pkCSM web server [55]. [b] Semaphore flags: green = good, yellow = tolerable, red = bad. [b] Unimportant, because the total clearance is high.

The volume of distribution (VD_{ss}) and fraction unbound are two of the most important pharmacokinetic drug parameters. Values of the VD_{ss} > 0.45 indicate that the drug will be distributed in tissue whereas values < −0.15 indicate that the drug will be distributed in plasma. So, VD_{ss} describes the extent of drug distribution, and the fraction unbound describes the portion of free drug in plasma

that may extravasate. Except for compounds 3164, the other ones showed almost intermediate values of VD_{ss}, and should have an adequate plasma distribution profile, with a fraction of the unbound drug between 0 and 0.157. These values indicate that the molecules can be well distributed and present a significative unbound fraction in the plasma, thus becoming available to interact with the pharmacological target. Only compound 3164 is entirely unable to penetrate the central nervous system (CNS).

The predicted values of the total clearance (Table 3), that measure the efficiency of the body in eliminating a drug, indicate that all compounds have a good renal elimination (1.5–8.4 mL/min/kg) and are not substrates of the renal organic cation transporter 2 (OCT2), with the exception of compound 13575. Finally, compounds 2076 and 14123 not passed the AMES and Minnow toxicity tests, respectively, whereas all others do not present any particular toxicity problems.

The overall lecture of Table 3 highlights that compounds 5339, 13575, and 1534 could be excellent candidates as drugs or, however, leads to further studies and manipulations.

3. Materials and Methods

3.1. Dataset of compounds

The chemical structures of the marine dataset were retrieved from Marine Natural Products (MNP, http://docking.umh.es/). The full list of the 2,922 molecules that passed the first statistical filter, including the MNP ID, SMILES, ligand-, and structural-based evaluation results, are available in the supplementary material (Table S1).

3.2. Structures preparation and minimization

The structures of all the molecules used in this study were built using Marvin Sketch (18.24, ChemAxon Ltd., Budapest, Hungary) [56]. A first molecular mechanics energy minimization was used for 3D structures created from the SMLES; the Merck molecular force field (MMFF94) present in Marvin Sketch [56] was used. The protonation states were calculated assuming a neutral pH. The PM3 Hamiltonian as implemented in MOPAC package (MOPAC2016 v. 18.151, Stewart Computational Chemistry, Colorado Springs, CO, USA) [57-59] was then used to further optimize the 3D structures before the alignment for the 3D-QSAR filter and the docking calculations.

3.3. Compound alignment for the 3D-ligand based filter

The alignment and evaluation of the 2,922 selected marine products were performed as follow. Firstly, the 3D structures of the molecules were imported into the software Forge (v10.4.2, Cresset, New Cambridge House, Hertfordshire, UK). The molecules were then aligned by a maximum common substructure algorithm using a customized and validated set-up [20, 22, 60], in the FABP4 3D-QSAR model already published by us [28, 29]. Before the alignment, the filed points of each molecule were generated using the XED (extended electron distribution) force field in Forge. The conformational analysis was done using a maximum number of 500 conformers using a gradient cutoff for conformer minimization of 0.1 kcal/mol and a similarity threshold, below which two conformers are assumed identical, of 0.5 Å. The energy window was set to 2.5 kcal/mol, and all the conformers with calculated energy outside the selected energy window were discarded.

3.4. Molecular docking

Molecular docking was performed using the three-dimensional crystal structure of substrate-free fatty acid-binding protein 4 in complex with BMS309403 (PDB ID: 2NNQ) obtained from the Protein Data Bank (PDB, http://www.rcsb.org/pdb). AutoDock Vina (v. 1.1.2, Molecular Graphics Lab at The Scripps Research Institute, La Jolla, California) [36], under the YASARA interface, was used for all docking experiments. All crystallographic water and SO_4^{2-} buffer molecules and ions were removed. Pearson's correlation coefficient method was used to validate the correspondence between the experimental pK_i values and the calculated ones from docking scores, utilizing a benchmark data

set of 34 known FABP4 inhibitors possessing pK_i values in the range of 1–5000 nM, to be reliable, chosen from those reported in the reference [17] (Table S1).

3.5. In silico ADMET studies

In silico molecular studies were conducted with the use of SwissADME [47] and pkCSM [55] web platforms.

4. Conclusions

Here, we described the screening of a collection of marine compounds retrieved from the MNP database in search of new potentially active FABP4 inhibitors. The whole dataset was first filtered using a statistical filter, employing 2D and 3D descriptors, and then the 2,992 filtered molecules were further evaluated in both a ligand- and a structure-based approach. For the ligand-based evaluation, we used an already successful implemented 3D-QSAR model for FABP4, whereas, for the structure-based, a docking analysis was performed. The results of both filters were then crossed between them for the 5% more active molecules, highlighting seven compounds possessing a calculated mean activity in the range of 79–245 nM. Interestingly, some of these seven compounds have already been tested for their cytotoxicity, and for anti-inflammatory actions, that could also be due to their activity in the FABP4 inhibition.

These seven compounds represent a good starting point for the discovery of novel potent and selective FABP4 inhibitors from natural products; in particular, compounds 5339, 13575, and 1534 possess very good predicted ADMET properties which make them excellent candidates for becoming new drugs. There is now the need for further *in vitro* and/or *in vivo* studies of these marine compounds to experimentally confirm their activity as FABP4 inhibitors. Furthermore, the extension of our research to other compounds (with high-expected activities) in Table S1 would also be a way to go.

Supplementary Materials: The following are available online, Table S1: Chemical structures of the FABP4 inhibitors used as benchmark for docking methodology validation, including both experimental and calculated pK_i binding affinities, Figure S1: Linear regression plot of experimental *vs*. calculated pK_i values reported in Table S1, Figure S2: Docking binding pose of 5339, Figure S2: Docking binding pose of 14123, Figure S3: Docking binding pose of 13575, Figure S4: Docking binding pose of 7846, Figure S5: Docking binding pose of 3164, Figure S6: Docking binding pose of 2076, Figure S7: Docking binding pose of 1534, Table S1: Chemical structures of the marine dataset that passed the first statistical filter including the ligand- (pIC_{50}) and structure-based (pK_i) calculated binding affinity.

Author Contributions: Conceptualization, G.F. and A.R.; methodology, G.F., D.G, V.P, and A.R; software, D.G and V.P; validation, G.F., D.G. and A.R.; formal analysis, G.F., D.G., G.P. and V.P.; investigation, G.F., D.G. and V.P.; resources, G.F., D.G., G.P. and A.R.; data curation, G.F., D.G. and A.R.; writing—original draft preparation, G.F., D.G. and A.R.; writing—review and editing, G.F., D.G., G.P., V.P. and A.R.; supervision, G.F. and A.R.; project administration, G.F. and A.R.

Funding: This research received no external funding.

Acknowledgments: We gratefully acknowledge Cresset and ChemAxon for the academic licenses for their software.

Conflicts of Interest: The authors declare no conflict of interest.

References

1. Das, U. N., Essential Fatty acids - a review. *Curr. Pharm. Biotechnol.* **2006**, 7, 467-482.
2. Boden, G., Free fatty acids (FFA), a link between obesity and insulin resistance. *Front. Biosci.* **1998**, 3, d169-175.
3. DeFronzo, R. A., Dysfunctional fat cells, lipotoxicity and type 2 diabetes. *Int. J. Clin. Pract. Suppl.* **2004**, 9-21.
4. Sheth, S. G.; Gordon, F. D.; Chopra, S., Nonalcoholic steatohepatitis. *Ann. Intern. Med.* **1997**, 126, 137-145.
5. Boden, G., Obesity and free fatty acids. *Endocrinol. Metab. Clin. North Am.* **2008**, 37, 635-646, viii-ix.

6. Storch, J.; Thumser, A. E., The fatty acid transport function of fatty acid-binding proteins. *Biochim. Biophys. Acta* **2000**, 1486, 28-44.
7. Queipo-Ortuno, M. I.; Escote, X.; Ceperuelo-Mallafre, V.; Garrido-Sanchez, L.; Miranda, M.; Clemente-Postigo, M.; Perez-Perez, R.; Peral, B.; Cardona, F.; Fernandez-Real, J. M.; Tinahones, F. J.; Vendrell, J., FABP4 dynamics in obesity: discrepancies in adipose tissue and liver expression regarding circulating plasma levels. *PLoS One* **2012**, 7, e48605.
8. Thompson, B. R.; Mazurkiewicz-Munoz, A. M.; Suttles, J.; Carter-Su, C.; Bernlohr, D. A., Interaction of Adipocyte Fatty Acid-binding Protein (AFABP) and JAK2 AFABP/aP2 AS A REGULATOR OF JAK2 SIGNALING. *J. Biol. Chem.* **2009**, 284, 13473-13480.
9. Adida, A.; Spener, F., Adipocyte-type fatty acid-binding protein as inter-compartmental shuttle for peroxisome proliferator activated receptor gamma agonists in cultured cell. *Biochimica Et Biophysica Acta-Molecular and Cell Biology of Lipids* **2006**, 1761, 172-181.
10. Fu, Y.; Luo, N.; Lopes-Virella, M. F.; Garvey, W. T., The adipocyte lipid binding protein (ALBP/aP2) gene facilitates foam cell formation in human THP-1 macrophages. *Atherosclerosis* **2002**, 165, 259-269.
11. Fu, Y.; Luo, L.; Luo, N.; Garvey, W. T., Lipid metabolism mediated by adipocyte lipid binding protein (ALBP/aP2) gene expression in human THP-1 macrophages. *Atherosclerosis* **2006**, 188, 102-111.
12. Nieman, K. M.; Kenny, H. A.; Penicka, C. V.; Ladanyi, A.; Buell-Gutbrod, R.; Zillhardt, M. R.; Romero, I. L.; Carey, M. S.; Mills, G. B.; Hotamisligil, G. S.; Yamada, S. D.; Peter, M. E.; Gwin, K.; Lengyel, E., Adipocytes promote ovarian cancer metastasis and provide energy for rapid tumor growth. *Nat. Med.* **2011**, 17, 1498-1503.
13. Tolle, A.; Suhail, S.; Jung, M.; Jung, K.; Stephan, C., Fatty acid binding proteins (FABPs) in prostate, bladder and kidney cancer cell lines and the use of IL-FABP as survival predictor in patients with renal cell carcinoma. *BMC Cancer* **2011**, 11, 302.
14. Uehara, H.; Takahashi, T.; Oha, M.; Ogawa, H.; Izumi, K., Exogenous fatty acid binding protein 4 promotes human prostate cancer cell progression. *Int. J. Cancer* **2014**, 135, 2558-2568.
15. Yang, A.; Zhang, H.; Sun, Y.; Wang, Y.; Yang, X.; Yang, X.; Zhang, H.; Guo, W.; Zhu, G.; Tian, J.; Jia, Y.; Jiang, Y., Modulation of FABP4 hypomethylation by DNMT1 and its inverse interaction with miR-148a/152 in the placenta of preeclamptic rats and HTR-8 cells. *Placenta* **2016**, 46, 49-62.
16. Lee, D.; Wada, K.; Taniguchi, Y.; Al-Shareef, H.; Masuda, T.; Usami, Y.; Aikawa, T.; Okura, M.; Kamisaki, Y.; Kogo, M., Expression of fatty acid binding protein 4 is involved in the cell growth of oral squamous cell carcinoma. *Oncol. Rep.* **2014**, 31, 1116-1120.
17. Floresta, G.; Pistarà, V.; Amata, E.; Dichiara, M.; Marrazzo, A.; Prezzavento, O.; Rescifina, A., Adipocyte fatty acid binding protein 4 (FABP4) inhibitors. A comprehensive systematic review. *Eur J Med Chem* **2017**, 138, 854-873.
18. Wang, Y.; Law, W. K.; Hu, J. S.; Lin, H. Q.; Ip, T. M.; Wan, D. C., Discovery of FDA-approved drugs as inhibitors of fatty acid binding protein 4 using molecular docking screening. *J. Chem. Inf. Model.* **2014**, 54, 3046-3050.
19. Zhou, Y.; Nie, T.; Zhang, Y.; Song, M.; Li, K.; Ding, M.; Ding, K.; Wu, D.; Xu, Y., The discovery of novel and selective fatty acid binding protein 4 inhibitors by virtual screening and biological evaluation. *Bioorg Med Chem* **2016**.
20. Floresta, G.; Apirakkan, O.; Rescifina, A.; Abbate, V., Discovery of High-Affinity Cannabinoid Receptors Ligands through a 3D-QSAR Ushered by Scaffold-Hopping Analysis. *Molecules* **2018**, 23.
21. Floresta, G.; Pittalà, V.; Sorrenti, V.; Romeo, G.; Salerno, L.; Rescifina, A., Development of new HO-1 inhibitors by a thorough scaffold-hopping analysis. *Bioorg Chem* **2018**, 81, 334-339.
22. Floresta, G.; Amata, E.; Dichiara, M.; Marrazzo, A.; Salerno, L.; Romeo, G.; Prezzavento, O.; Pittalà, V.; Rescifina, A., Identification of Potentially Potent Heme Oxygenase 1 Inhibitors through 3D-QSAR Coupled to Scaffold-Hopping Analysis. *ChemMedChem* **2018**, 13, 1336-1342.
23. Salerno, L.; Amata, E.; Romeo, G.; Marrazzo, A.; Prezzavento, O.; Floresta, G.; Sorrenti, V.; Barbagallo, I.; Rescifina, A.; Pittalà, V., Potholing of the hydrophobic heme oxygenase-1 western region for the search of potent and selective imidazole-based inhibitors. *Eur J Med Chem* **2018**, 148, 54-62.
24. Floresta, G.; Rescifina, A.; Marrazzo, A.; Dichiara, M.; Pistarà, V.; Pittalà, V.; Prezzavento, O.; Amata, E., Hyphenated 3D-QSAR statistical model-scaffold hopping analysis for the identification of potentially potent and selective sigma-2 receptor ligands. *Eur J Med Chem* **2017**, 139, 884-891.

25. Rescifina, A.; Floresta, G.; Marrazzo, A.; Parenti, C.; Prezzavento, O.; Nastasi, G.; Dichiara, M.; Amata, E., Sigma-2 receptor ligands QSAR model dataset. *Data Brief* **2017**, 13, 514-535.
26. Rescifina, A.; Floresta, G.; Marrazzo, A.; Parenti, C.; Prezzavento, O.; Nastasi, G.; Dichiara, M.; Amata, E., Development of a Sigma-2 Receptor affinity filter through a Monte Carlo based QSAR analysis. *Eur J Pharm Sci* **2017**, 106, 94-101.
27. Floresta, G.; Rescifina, A.; Abbate, V., Structure-Based Approach for the Prediction of Mu-opioid Binding Affinity of Unclassified Designer Fentanyl-Like Molecules. *Int J Mol Sci* **2019**, 20.
28. Floresta, G.; Cilibrizzi, A.; Abbate, V.; Spampinato, A.; Zagni, C.; Rescifina, A., FABP4 inhibitors 3D-QSAR model and isosteric replacement of BMS309403 datasets. *Data Brief* **2019**, 22, 471-483.
29. Floresta, G.; Cilibrizzi, A.; Abbate, V.; Spampinato, A.; Zagni, C.; Rescifina, A., 3D-QSAR assisted identification of FABP4 inhibitors: An effective scaffold hopping analysis/QSAR evaluation. *Bioorg. Chem.* **2019**, 84, 276-284.
30. Floresta, G.; Amata, E.; Barbaraci, C.; Gentile, D.; Turnaturi, R.; Marrazzo, A.; Rescifina, A., A Structure- and Ligand-Based Virtual Screening of a Database of "Small" Marine Natural Products for the Identification of "Blue" Sigma-2 Receptor Ligands. *Mar Drugs* **2018**, 16.
31. Floresta, G.; Amata, E.; Gentile, D.; Romeo, G.; Marrazzo, A.; Pittalà, V.; Salerno, L.; Rescifina, A., Fourfold Filtered Statistical/Computational Approach for the Identification of Imidazole Compounds as HO-1 Inhibitors from Natural Products. *Mar Drugs* **2019**, 17.
32. Sander, T.; Freyss, J.; von Korff, M.; Rufener, C., DataWarrior: an open-source program for chemistry aware data visualization and analysis. *J. Chem. Inf. Model.* **2015**, 55, 460-473.
33. Cheeseright, T.; Mackey, M.; Rose, S.; Vinter, A., Molecular field extrema as descriptors of biological activity: definition and validation. *J Chem Inf Model* **2006**, 46, 665-676.
34. Cai, H.; Liu, Q.; Gao, D.; Wang, T.; Chen, T.; Yan, G.; Chen, K.; Xu, Y.; Wang, H.; Li, Y.; Zhu, W., Novel fatty acid binding protein 4 (FABP4) inhibitors: virtual screening, synthesis and crystal structure determination. *Eur. J. Med. Chem.* **2015**, 90, 241-250.
35. Cai, H.; Yan, G.; Zhang, X.; Gorbenko, O.; Wang, H.; Zhu, W., Discovery of highly selective inhibitors of human fatty acid binding protein 4 (FABP4) by virtual screening. *Bioorg. Med. Chem. Lett.* **2010**, 20, 3675-3679.
36. Trott, O.; Olson, A. J., AutoDock Vina: improving the speed and accuracy of docking with a new scoring function, efficient optimization, and multithreading. *J Comput Chem* **2010**, 31, 455-461.
37. Yao, S.; Gallenkamp, D.; Wolfel, K.; Luke, B.; Schindler, M.; Scherkenbeck, J., Synthesis and SERCA activities of structurally simplified cyclopiazonic acid analogues. *Bioorg Med Chem* **2011**, 19, 4669-4678.
38. Kobayashi, M.; Lee, N. K.; Son, B. W.; Yanag, K.; Kyogoku, Y.; Kitagawa, I., Stoloniferone-a, -b, -c, and -d, four new cytotoxic steroids from the okinawan soft coral clavularia viridis. *Tetrahedron Lett* **1984**, 25, 5925-5928.
39. Rudi, A.; Erez, Y.; Benayahu, Y.; Kashman, Y., Omriolide A and B; two new rearranged spongian diterpenes from the marine sponge Dictyodendrilla aff. retiara. *Tetrahedron Lett* **2005**, 46, 8613-8616.
40. Iwashima, M.; Matsumoto, Y.; Takenaka, Y.; Iguchi, K.; Yamori, T., New marine diterpenoids from the Okinawan soft coral Clavularia koellikeri. *J Nat Prod* **2002**, 65, 1441-1446.
41. Kobayashi, J. i.; Hirase, T.; Shigemori, H.; Ishibashi, M.; Bae, M.-A.; Tsuji, T.; Sasaki, T., New Pentacyclic Compounds from the Okinawan Marine Sponge Xestospongia sapra. *Journal of Natural Products* **1992**, 55, 994-998.
42. Delfourne, E.; Bastide, J., Marine pyridoacridine alkaloids and synthetic analogues as antitumor agents. *Med Res Rev* **2003**, 23, 234-252.
43. Motti, A. C.; Bourguet-Kondracki, M.-L.; Longeon, A.; Doyle, R. J.; Llewellyn, E. L.; Tapiolas, M. D.; Yin, P., Comparison of the Biological Properties of Several Marine Sponge-Derived Sesquiterpenoid Quinones. *Molecules* **2007**, 12.
44. Khanaki, K.; Sadeghi, M. R.; Akhondi, M. M.; Darabi, M.; Mehdizadeh, A.; Shabani, M.; Rahimipour, A.; Nouri, M., High ω-3:ω-6 fatty acids ratio increases fatty acid binding protein 4 and extracellular secretory phospholipase A2IIa in human ectopic endometrial cells. *ijrm* **2014**, 12, 755-750.
45. Wang, Y.; Lin, H.-Q.; Xiao, C.-Y.; Law, W.-K.; Hu, J.-S.; Ip, T.-M.; Wan, D. C.-C., Using molecular docking screening for identifying hyperoside as an inhibitor of fatty acid binding protein 4 from a natural product database. *J Funct Foods* **2016**, 20, 159-170.
46. Matlock, M. K.; Hughes, T. B.; Dahlin, J. L.; Swamidass, S. J., Modeling Small-Molecule Reactivity Identifies Promiscuous Bioactive Compounds. *J. Chem. Inf. Model.* **2018**, 58, 1483-1500.

406 47. Daina, A.; Michielin, O.; Zoete, V., SwissADME: a free web tool to evaluate pharmacokinetics, drug-likeness
407 and medicinal chemistry friendliness of small molecules. *Scientific Reports* **2017**, 7.
408 48. Lipinski, C. A.; Lombardo, F.; Dominy, B. W.; Feeney, P. J., Experimental and computational approaches to
409 estimate solubility and permeability in drug discovery and development settings. *Adv. Drug Delivery. Rev.*
410 **1997**, 23, 3-25.
411 49. Ghose, A. K.; Viswanadhan, V. N.; Wendoloski, J. J., A knowledge-based approach in designing
412 combinatorial or medicinal chemistry libraries for drug discovery. 1. A qualitative and quantitative
413 characterization of known drug databases. *J. Comb. Chem.* **1999**, 1, 55-68.
414 50. Egan, W. J.; Merz, K. M.; Baldwin, J. J., Prediction of drug absorption using multivariate statistics. *J. Med.*
415 *Chem.* **2000**, 43, 3867-3877.
416 51. Veber, D. F.; Johnson, S. R.; Cheng, H. Y.; Smith, B. R.; Ward, K. W.; Kopple, K. D., Molecular properties that
417 influence the oral bioavailability of drug candidates. *J. Med. Chem.* **2002**, 45, 2615-2623.
418 52. Muegge, I.; Heald, S. L.; Brittelli, D., Simple selection criteria for drug-like chemical matter. *J. Med. Chem.*
419 **2001**, 44, 1841-1846.
420 53. Teague, S. J.; Davis, A. M.; Leeson, P. D.; Oprea, T., The design of leadlike combinatorial libraries. *Angewandte*
421 *Chemie-International Edition* **1999**, 38, 3743-3748.
422 54. Baell, J. B.; Holloway, G. A., New Substructure Filters for Removal of Pan Assay Interference Compounds
423 (PAINS) from Screening Libraries and for Their Exclusion in Bioassays. *J. Med. Chem.* **2010**, 53, 2719-2740.
424 55. Pires, D. E. V.; Blundell, T. L.; Ascher, D. B., pkCSM: Predicting Small-Molecule Pharmacokinetic and
425 Toxicity Properties Using Graph-Based Signatures. *J. Med. Chem.* **2015**, 58, 4066-4072.
426 56. Barf, T.; Lehmann, F.; Hammer, K.; Haile, S.; Axen, E.; Medina, C.; Uppenberg, J.; Svensson, S.; Rondahl, L.;
427 Lundback, T., N-Benzyl-indolo carboxylic acids: Design and synthesis of potent and selective adipocyte fatty-
428 acid binding protein (A-FABP) inhibitors. *Bioorg. Med. Chem. Lett.* **2009**, 19, 1745-1748.
429 57. Stewart, J. J. P., Optimization of parameters for semiempirical methods IV: extension of MNDO, AM1, and
430 PM3 to more main group elements. *J. Mol. Model.* **2004**, 10, 155-164.
431 58. Alemán, C.; Luque, F. J.; Orozco, M., Suitability of the PM3-derived molecular electrostatic potentials. *J.*
432 *Comput. Chem.* **1993**, 14, 799-808.
433 59. Qiao, F.; Luo, L.; Peng, H.; Luo, S.; Huang, W.; Cui, J.; Li, X.; Kong, L.; Jiang, D.; Chitwood, D. J.; Peng, D.,
434 Characterization of Three Novel Fatty Acid- and Retinoid-Binding Protein Genes (Ha-far-1, Ha-far-2 and Hf-
435 far-1) from the Cereal Cyst Nematodes Heterodera avenae and H. filipjevi. *PLoS One* **2016**, 11, e0160003.
436 60. Floresta, G.; Rescifina, A.; Marrazzo, A.; Dichiara, M.; Pistarà, V.; Pittalà, V.; Prezzavento, O.; Amata, E.,
437 Hyphenated 3D-QSAR statistical model-scaffold hopping analysis for the identification of potentially potent
438 and selective sigma-2 receptor ligands. *Eur. J. Med. Chem.* **2017**, 139, 884-891.
439